Ceramics International 23 (1997) 367–373

PII: S0272-8842(96)00045-4
0272-8842/97 $17.00+0.00

Ultrasonic Testing of Artificial Defects in Alumina Ceramic

Li-Shin Chang* & Tung-Han Chuang

Institute of Materials Science and Engineering, National Taiwan University, Taipei, Taiwan

(Received 1 November 1995; accepted 18 January 1996)

Abstract: This research tried to correlate the defect diameter and the ultrasonic signal reflected from the interface between an alumina matrix and artificial cylinder-like defects. Some fundamental acoustic and geometrical equations were used to determine the diameter from some known or pre-measured parameters. A final comparison between the real and predicted defect diameter was made to check out the accuracy of the model. The error of the size prediction of a solid defect was smaller than 65% in 10 MHz ultrasonic testing and even smaller than 15% when the defect type was a hole. The influence of the defect diameter on the prediction was dependent on the shrinkage of the specimens. We also found that the best density for ultrasonic testing was around 3.8 gm/cm^3. © 1997 Elsevier Science Limited and Techna S.r.l.

Keywords: alumina, ultrasonic testing, artificial defects.

1 INTRODUCTION

Ceramics are usually very sensitive to cracks because of their poor toughness. Therefore, unreliable specimen preparation may violently change the properties of ceramics. Non-destructive testing (NDT) methods can avoid most of the disadvantages of destructive testing, and especially ultrasonic testing (UT) has received the most attention in the last few years.[1,2] Not only is it economical and reliable, but it also has a large field of application, a wide range of detectable defect types and strong penetration ability. In the applicability of ultrasonic testing on flaw defects, Sokolov in 1929 measured the reduction of the echo intensity to identify the location of defects. In 1942, Firestone applied the ultrasonic technique, used in locating ships and measuring ocean depths, to materials. After 1945, most of the applications on metallic materials, for example, measurements of sound velocity, thickness, defects, mechanical properties, etc., were standardized. However, there has been little research on ceramics because of the difficulty in producing the standard specimens. Kino[3] has estimated defects in ceramics using high frequency UT. Khuri-Yakub *et al.*[4] have used acoustic surface waves to measure surface cracks in ceramics. Hefetz and Rokhlin[5] have also estimated thermal shock damage by using ultrasonic waves to detect surface microcracks. In this research, we placed some wires into alumina and then found the relation between the ultrasonic signal, especially that reflected by the intrinsic defects, and the actual defect size which was observed by cutting open the specimens.

*Present address: Institut für Metallkunde, Universität Stuttgart, Seestr. 75, 70174, Stuttgart, Germany

2 EXPERIMENTAL PROCEDURE

2.1 The preparation of alumina samples

Platinum and nylon wires with diameters of 100, 300 and 500 μm as cylinder-like defects were put into ceramic disks while they were being formed from alumina slurry by pressure slip casting in two steps, which means that at first we cast only half of the slurry, poured out another half slurry from the mould, put the wire on the surface of the half cake, and then continued to cast the other half of the

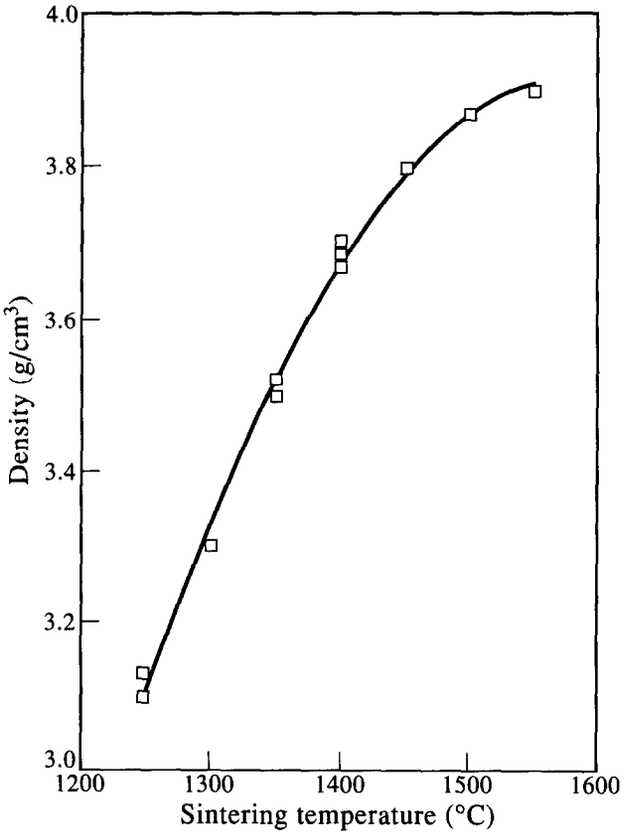

Fig. 1. The curve of densities related to sintering temperatures.

slurry until all of the slurry was cast. The slurry consisted of 50 wt% Al_2O_3 powder and 0.5 wt% Darvan C as dispersant and binder. The duration of forming was 30 min. under a uniaxial pressure of 10 kg/cm^2 when 20 ml slurry was cast. The diameters of the green cakes were 25 mm. The thickness of the green cakes was 10 mm. After 24 h of drying at 60 °C, these green cakes were then sintered in air under temperatures of 1250, 1350, 1450 and 1550 °C for 2 h to produce ceramics with different densities, as shown in Fig. 1. These bulk densities were measured by means of the Archimedes method.[6] The sintered ceramic specimens were finally ground using a 500# diamond grinding wheel with a grinding rate of 0.02–0.04 mm/cycle.

2.2 The ultrasonic testing of alumina

The adopted ultrasonic testing equipment included a USIP 12 and DTM 12 made by the Krautkramer–Branson Corp. The transducer was unfocused and contacted the surfaces of the specimens with a couplant. The mode of ultrasonic testing adopted in this work was the A-scan mode. All of these experimental conditions are set for the purpose of simplifying the model for predicting the wire

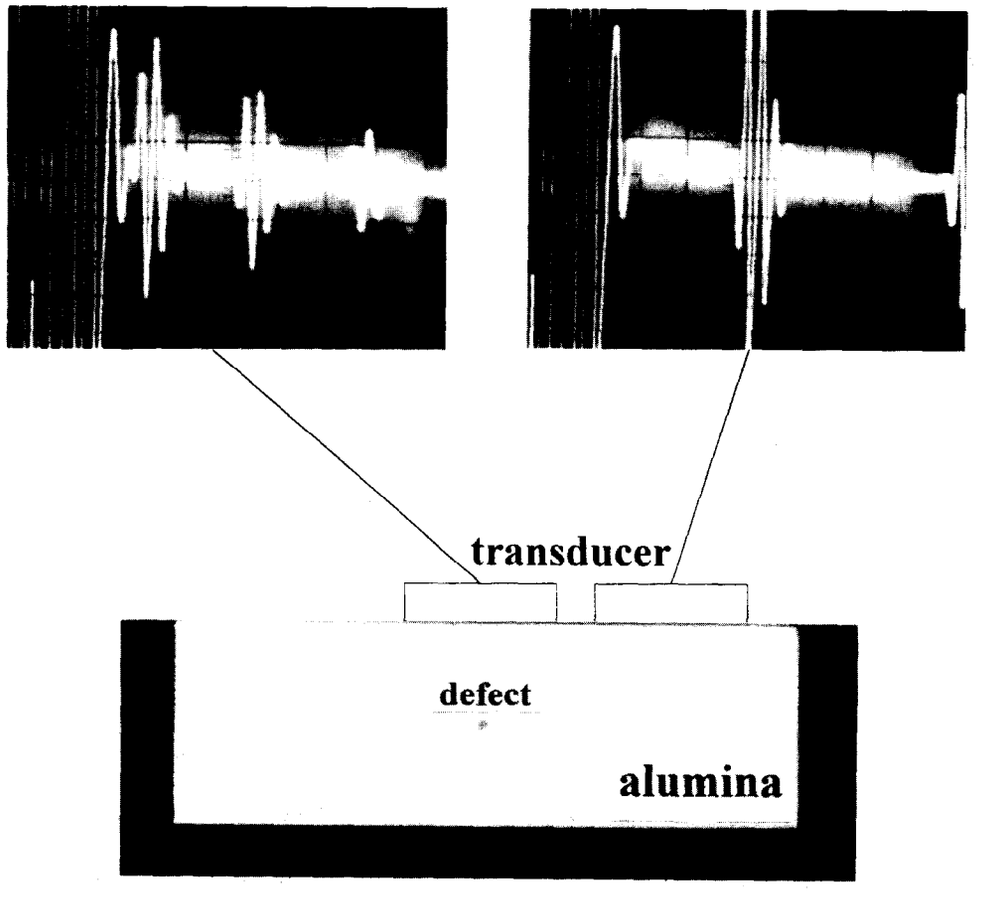

Fig. 2. Ultrasonic signals and their relative position in a specimen.

diameter. We chose 10 MHz as the testing frequency and glycerine as the couplant. Two parameters, (1) the time difference between two echoes (Δt) and (2) the amplitudes of the back echoes (P_b) and defect echoes (P_d), were recorded. An example of ultrasonic signals and their relative positions in a specimen is shown in Fig. 2. To confirm the defect entirely within the testing area of the transducer, the maximum defect echo amplitude was recorded during movement of the transducer along the surface of the specimens. After ultrasonic testing, the specimens were cut along the cross-section of defects. The real defect diameters were measured directly from the observed embedded defects in the ceramics as shown in Fig. 3.

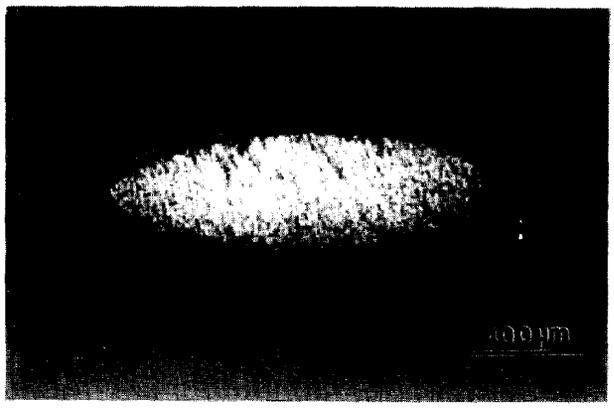

a.

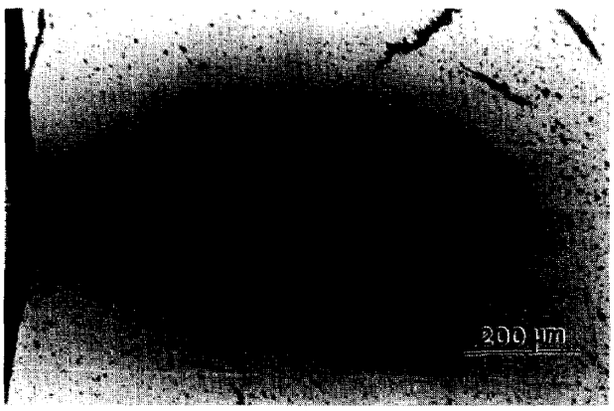

b.

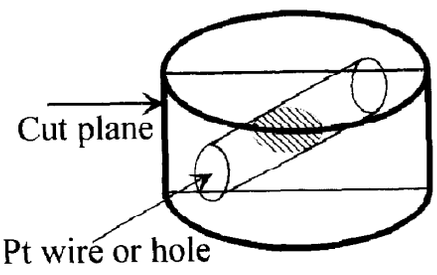

c.

Fig. 3. The cross-section of (a) the platinum wire; (b) the hole embedded in the alumina and (c) the schematic diagram.

3 THEORY BACKGROUND

A pulse is transmitted into the matrix, and a part of it is reflected from the curve interface on a defect. Besides the attenuation caused by scattering and absorption in grains and grain boundaries,[7] there are several phenomena which need to be considered in estimating the cylinder's diameter from the echo amplitude.[8] The description equations of these phenomena are presented as follows:

3.1 Sound pressure (P) at some point along the axis of the transducer:[9]

$$P = 2P_0 \sin[(\sqrt{R^2 + a^2} - a)\frac{\pi}{\lambda}] = k_1 P_0 \tag{1}$$

where P_0 is the initial pressure, R the transducer radius, a the axial distance between the point and the transducer, and λ the wavelength.

3.2 Surface curvature effect of defects:

$$P = k_1 P_0 \sqrt{\frac{D}{2(1+\frac{x}{a})[x + f(1+\frac{x}{a})]}} = k_1 k_2 P_0, \tag{2}$$

where a is the distance between the sound source and the curve surface, x the distance between some point and the curve surface, and D the defect diameter.

3.3 Length of defects:

$$P = P_0[1 - (\frac{2}{\pi}\cos^{-1}\frac{L}{2R} - \frac{L}{2\pi R}\sqrt{1 - \frac{L^2}{4R^2}})] = k_3 P_0, \tag{3}$$

where L is the defect length, R the transducer radius and k_3 the effected area ratio.

3.4 First reflection factor (I) in interfaces:[10]

$$\text{from front interface } I_1 = \frac{Z_d - Z_m}{Z_d + Z_m} \tag{4}$$

$$\text{from back interface } I_2 = \frac{4Z_d Z_m (Z_d - Z_m)}{(Z_d + Z_m)^3}, \tag{5}$$

where Z_d, Z_m are the impedances of the defect and the matrix. It is notable that I is very small and

negligible after second reflection, and that the wave transformation which occurs by propagating through a non-flat interface is assumed to be negligible to simplify the model. The measured wavelength in the alumina at a frequency of 10 MHz is about 100 μm, and the cylinder diameters are $n \times 100$ μm ($n = 1$, 3 or 5). That means the first reflections from the front and back interfaces have the same phase. The factor (k_4) can be simply expressed by adding I_1 and I_2.

Combining all of these equations, the relation between the reflected sound pressure and initial pressure can be described as a function of defect diameter and defect depth:

$$P = k_1 k_2 k_3 k_4 P_0 e^{\alpha x} = f(D, x, \alpha) P_0. \quad (6)$$

After measuring the defect depth (x) which was calculated from $v \times \Delta t$ (v: sound velocity in specimen and $v = \frac{2d}{\Delta t_0}$, d: specimen thickness; Δt_0: time difference between two back echoes from the bottom) and the attenuation coefficient (α), which was approximately calculated from P_b, the cylinder diameter (D) can be solved for when P_d/P_b is known. As a comparison, we adopted the experience relation suitable for a cylinder hole:

$$\frac{P_d}{P_0} = \frac{kL\sqrt{D\lambda}}{2\pi R^2}, \quad (7)$$

where P_d, P_0 are the amplitudes of the defect echo and initial pulse, L, D the length and diameter of the hole, R the radius of the transducer, and λ the wavelength.

4 RESULTS AND DISCUSSION

The wavelength, defect depth and attenuation coefficient measured from the pulse echoes and the defect diameters through ultrasonic determination and metallographic observation are summarized in Table 1. The defect diameter calculated from eqn (6) better matched the true value observed by using an optical microscope than did that from eqn (7). The error from the experience equation could be as much as 188%. The errors from eqn (6) which we established were less than 65%. Figure 4 shows that the influence of the defect type (solid or hole) was different with the same defect length. The prediction error of hole defects (made from nylon wire) decreased to the hole radius, while that of a solid defect embedded with platinum wire deceased firstly with defect size and then increased with a minimum at $D \approx 300$ μm. This may be attributable to the residual stress region formed during sintering. At first, concerning the residual stress region, it is apparent to imagine that the accuracy of predicting the platinum radius should decrease with the density when a homogenous green cake was considered. But, in fact, the real correlation as shown in Fig. 5 is more complicated than that. The ideal consideration fitted only when the platinum radii were about 500 μm. The errors changed

Table 1. Parameters of specimens and the defect diameters measured and predicted and their errors

	No.	λ (μm)	x (μm)	α (Np/μm)	P_d/P_b (%)	L (mm)	D_0^* (μm)	D_1^* (μm)	D_{2a}^* (μm)	D_{2b}^* (μm)	E_{2a}^* (%)	E_{2b}^* (%)
Pt	1	110	3409	39	10.6	5	500	430	710	726	65	69
	2	109	3550	51	6.4	5	300	280	282	267	1	5
	3	111	2962	35	6.8	5	100	98	110	75	12	23
	4	106	2002	41	4.4	5	500	430	484	506	13	18
	5	93	4005	54	11.5	5	500	435	620	451	43	4
	6	69	3533	45	21.1	5	500	430	556	1143	29	166
	7	109	2890	69	6.0	5	300	285	280	232	2	19
	8	90	3252	58	10.0	5	300	285	230	350	19	23
	9	70	2973	80	6.5	5	300	280	251	384	10	37
	10	108	1973	18	3.0	5	100	96	78	60	19	38
	11	92	2600	68	3.1	5	100	94	76	75	19	20
	12	68	2632	102	2.8	5	100	98	40	82	59	16
	13	112	2517	61	16.7	10	500	420	440	441	5	5
	14	113	2270	53	15.0	10	300	285	236	354	17	24
	15	112	2067	46	4.6	10	100	93	88	131	5	41
	16	111	4807	34	7.7	3	500	435	345	467	21	7
	17	110	4417	30	1.3	1	500	430	245	283	43	34
Hole	18	111	4065	24	15.7	5	500	350	384	394	10	13
	19	111	5249	30	26.3	5	300	230	254	662	10	188
	20	111	3887	29	4.6	5	100	98	112	137	14	40
	21	112	3736	32	4.0	5	500	435	464	281	7	35
	22	112	3517	36	4.5	5	500	430	426	357	1	17

*D_0: original wire diameter, D_1: metallographic observation, D_{2a}, E_{2a}, D_{2b}, E_{2b}: predictions (ultrasonic measured and calculated from eqns (6) and (7)).

slightly with density when the radius was about 300 μm. At about 100 μm, on the contrary, the errors were reduced with increasing density. This may be explained by a combination of two factors: the errors from the residual stress region (f_1) and the unavoidable artificial destruction during processing of the specimens (f_2). f_1 is about proportional to the square of the wire diameter (D) and the linear shrinkage of the matrix (δ). δ can be established from Fig. 2. f_2 decreased as the shrinkage increased. They can be expressed as follows:

$$f_1 = AD^2\delta, \tag{8}$$

$$f_2 = B(\delta_0 - \delta), \tag{9}$$

and so the error $E = \frac{f_1+f_2}{D}$, where A, B are constants. From Fig. 5, we assume that at $D = 500$, 300 and 100 μm the deviations of the error ($dE/d\delta$) are constants, and that they are m, 0 and n. From this assumption and eqns (8) and (9), we can obtain that $m/n \approx -0.4$. This is in agreement with the experimental data value of -0.32 (see Fig. 5). This means, although the scattering of the experimental errors is serious because the plane-wave theories are less suitable under small defect conditions, the trend of the course of errors is as predicted. It must be noted that the assumption $\frac{dE}{d\delta} \simeq$ const. is a rough estimate. The data in Fig. 5 suggest to us that the discontinuous location of the powder size distribution caused by two-step formation of the green cake could be eliminated when the density was higher than 3.5 g/cm^3; in other words, after sintering at temperatures higher than 1300 °C for 2 h, the optimal density for the ultrasonic testing was 3.8 g/cm^3. Now we consider the "C-curve" in Fig. 4. With deviation of the error to the diameter $\frac{dE}{dD}|_{D+D_0} = 0$, the equation

$$D_0 = \sqrt{\frac{B(\delta_0 - \delta)}{A\delta}}, \tag{10}$$

is obtained, where D_0 is the optimal defect diameter on which the error is a minimum. A and B are defined as in eqns (8) and (9). We obtain $D_0 = 72$, 106, 193 and 348 μm for different densities (3.9, 3.8, 3.5 and 3.1 g/cm^3), sintered at different temperatures (1550, 1450, 1350 and 1250 °C). From Fig. 4 the tendency shows that the optimal diameter of the minimum values of errors for ultrasonic testing decrease as the density increases. The correlation of eqn (10) and the experimental values fitted in Fig. 4 is shown in Fig. 6. Figure 7 shows the correlation between the error and the platinum

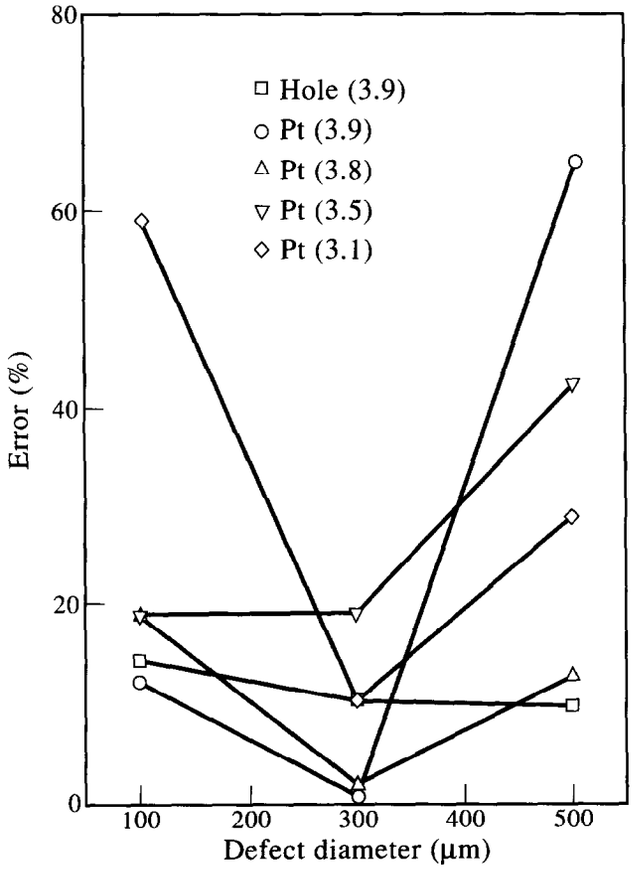

Fig. 4. The correlation between the error and the defect diameter. (...) bulk density of specimen, g/cm^3.

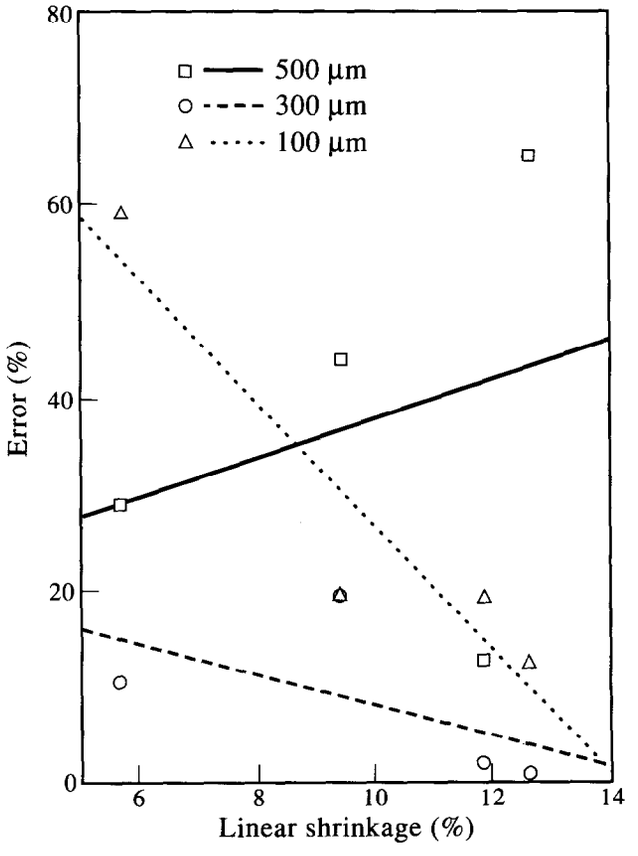

Fig. 5. The correlation between the error and the linear shrinkage.

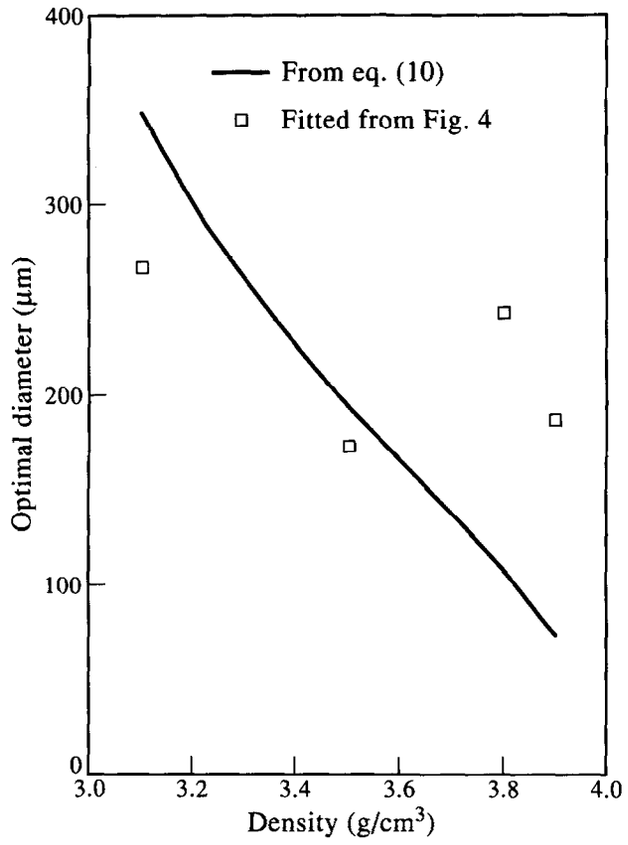

Fig. 6. The correlation between the optimal diameter and the density.

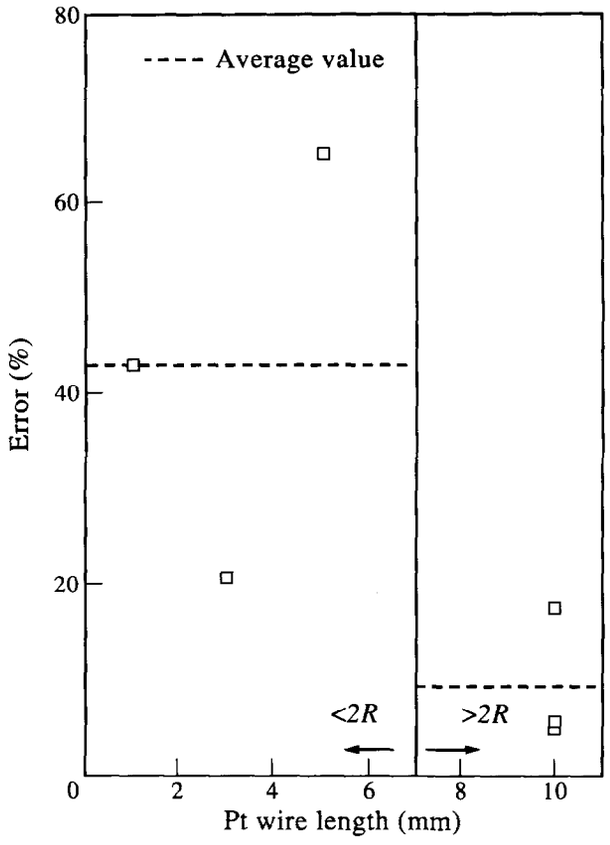

Fig. 7. The correlation between the error and the wire length. R is the transducer radius.

wire length with a diameter of 500 μm. The error was reduced to 2% when the length was 10 mm. Since the transducer diameter was 7 mm, eqn (3) had to be taken into consideration when the wire length was shorter than 7 mm. This may have introduced more errors into the theoretical model. The total error of eqn (3) was about $6\Delta L$ when the error of the length was ΔL. The experimental error in measuring the length was 5%, and the total error was about 30%. This agrees with the difference of the average values of two regions, 33.8 (see dotted lines in Fig. 7, 42.9 for $L < 7$ mm and 9.1 for $L > 7$ mm).

5 CONCLUSIONS

1. The prediction of defect diameters using the equations which describe briefly each phenomenon involved in wave propagation in an alumina bulk containing a cylinder-like defect was reliable, and the error was tolerably smaller than 65% when the defect diameter was in the range 500–100 μm.
2. Correlations between the error and the parameters, diameter, density, etc., have been found and explained well by introducing some simple sintering concepts. The optimal density for ultrasonic testing specimen was 3.8 g/cm^3 (sintered at 1450 °C for 2 h), and the obtained correlation between the density and the defect diameter on which the best accuracy was approximately linear.
3. The theoretical error found by introducing the factor of length explained well the error difference between the two defect length regions separated by 7 mm.

REFERENCES

1. ELLIGSON, W. A., ROBERTS, R. A., ACKERMAN, J. L., SAWICKA, B. D., GRONEMEYER, S. & KRITZ, J., Recent developments in nondestructive evaluation for structure ceramics. *Int. Adv. in Nondestructive Test.*, **13** (1987) 267–294.
2. DAVIDGE, R. W., Defects in ceramics — the targets for NDT. *Brit. Ceram. Trans. J.*, **88** (1989) 113–116.
3. KINO, G. S., The application of reciprocity theory to scattering of acoustic waves by flaws. *J. Appl. Phys.*, **49**(6) (1978) 3190–3199.
4. KHURI-YAKUB, B. T., KINO, G. S. & EVANS, A. G., Acoustic surface wave measurements of surface cracks in ceramics. *J. Am. Ceram. Soc.*, **63**(1) (1980) 65–71.
5. HEFETZ, M. & ROKHLIN, S. I., Thermal shock damage assessment in ceramics using ultrasonic waves. *J. Am. Ceram. Soc.*, **75**(7) (1992) 1839–1845.
6. PENNINGS, C. M. & GRELLNER, W., Precise nondestructive determination of the density of porous ceramics. *J. Am. Ceram. Soc.*, **71**(7) (1989) 1268–1279.

7. DANILOV, N., Calculation of the attenuation coefficient of elastic waves in scattering in polycrystalline media. *Trans. from Defectoskopiya*, **8** (1989) 18–23.
8. VOPILKIN, A.Kh., Methods of type recognition and measurement of defect dimensions in ultrasonic inspection (A review). *Soviet J. Nondestructive Testing*, (1990) 1–18.
9. ZHANG, Q., MA, T. & LIN, S., Detection of defects in ceramic materials by ultrasonic technique. *J. Inorg. Mater.*, **2**(4) (1987) 354–362.
10. VARY, A., Correlations among ultrasonic propagation factors and fracture toughness properties of metallic materials. *Mater. Eval.*, **36**(7) (1978) 55–64.